

**The OGLE Collection of Variable Stars.  
Over 15 000  $\delta$  Scuti Stars in the Large Magellanic Cloud\***

I. Soszyński<sup>1</sup>, P. Pietrukowicz<sup>1</sup>, A. Udalski<sup>1</sup>, J. Skowron<sup>1</sup>,  
M.K. Szymański<sup>1</sup>, R. Poleski<sup>1</sup>, D.M. Skowron<sup>1</sup>, S. Kozłowski<sup>1</sup>,  
P. Mróz<sup>1</sup>, P. Iwanek<sup>1</sup>, M. Wrona<sup>1</sup>, K. Ulaczyk<sup>2,1</sup>, K. Rybicki<sup>3,1</sup>,  
M. Gromadzki<sup>1</sup> and M. Mróz<sup>1</sup>

<sup>1</sup> Astronomical Observatory, University of Warsaw, Al. Ujazdowskie 4,  
00-478 Warszawa, Poland

<sup>2</sup> Department of Physics, University of Warwick, Gibbet Hill Road, Coventry,  
CV4 7AL, UK

<sup>3</sup> Department of Particle Physics and Astrophysics, Weizmann Institute of Science,  
Rehovot 76100, Israel

*Received September 26, 2023*

ABSTRACT

We present the OGLE collection of  $\delta$  Scuti stars in the Large Magellanic Cloud and in its foreground. Our dataset encompasses a total of 15 256 objects, constituting the largest sample of extragalactic  $\delta$  Sct stars published so far. In the case of 12  $\delta$  Sct pulsators, we detected additional eclipsing or ellipsoidal variations in their light curves. These are the first known candidates for binary systems containing  $\delta$  Sct components beyond the Milky Way. We provide observational parameters for all variables, including pulsation periods, mean magnitudes, amplitudes, and Fourier coefficients, as well as long-term light curves in the *I*- and *V*-bands collected during the fourth phase of the OGLE project.

We construct the period–luminosity (PL) diagram, in which fundamental-mode and first-overtone  $\delta$  Sct stars form two nearly parallel ridges. The latter ridge is an extension of the PL relation obeyed by first-overtone classical Cepheids. The slopes of the PL relations for  $\delta$  Sct variables are steeper than those for classical Cepheids, indicating that the continuous PL relation for first-overtone  $\delta$  Sct variables and Cepheids is non-linear, exhibiting a break at a period of approximately 0.5 d.

We also report the enhancement of the OGLE collection of Cepheids and RR Lyr stars with newly identified and reclassified objects, including pulsators contained in the recently published Gaia DR3 catalog of variable stars. As a by-product, we estimate the contamination rate in the Gaia DR3 catalogs of Cepheids and RR Lyr variables.

**Key words:** *Stars: variables: delta Scuti – Stars: oscillations – Magellanic Clouds – Catalogs*

---

\*Based on observations obtained with the 1.3-m Warsaw telescope at the Las Campanas Observatory of the Carnegie Institution for Science.

## 1. Introduction

The fourth phase of the Optical Gravitational Lensing Experiment (OGLE-IV) has yielded extensive catalogs of variable stars, including nearly complete samples of Cepheids and RR Lyr stars in the Magellanic Clouds (*e.g.*, Soszyński *et al.* 2015a, 2016, 2017, 2019).  $\delta$  Scuti variables share the same pulsation mechanism with Cepheids and RR Lyr stars, which consequently places them within the same instability strip in the Hertzsprung-Russell diagram. Recently, Soszyński *et al.* (2022) published a collection of over 2600  $\delta$  Sct pulsators in the Small Magellanic Cloud (SMC) – the first ever such catalog covering the entire area of this galaxy. In this paper, we extend the OGLE Collection of Variable Stars (OCVS) by about 15 000  $\delta$  Sct stars carefully selected in the OGLE-IV photometric database in the Large Magellanic Cloud (LMC).

$\delta$  Sct are mid-A to early-F type pulsating stars that populate the Cepheid instability strip on or slightly above the main sequence. They exhibit low-order radial and non-radial pressure modes with periods below 0.3 d that are self-excited through the  $\kappa$ -mechanism. The  $\delta$  Sct class includes a mixture of stars at different evolutionary stages: young stellar objects during their contraction toward the main sequence, stars with core hydrogen burning on the main sequence, subgiants evolving off the main sequence, and Population II blue stragglers, called SX Phe stars.

The first  $\delta$  Sct stars in the LMC were discovered 20 years ago. The OGLE-II catalog of RR Lyr stars in the LMC (Soszyński *et al.* 2003) was supplemented with 37 short-period pulsating variables, of which 29 turned out to be actual  $\delta$  Sct stars, while the remaining ones were ultimately classified as Cepheids or RR Lyr stars. In turn, Kaluzny and Rucinski (2003) reported the discovery of eight small-amplitude short-period variables in the LMC open cluster LW 55 and suggested that seven of them might be  $\delta$  Sct stars.

The largest catalogs of  $\delta$  Sct stars in the LMC to date were published based on photometric data collected by the OGLE-III, SuperMACHO, and EROS-2 surveys. Poleski *et al.* (2010) identified 2788 candidates for  $\delta$  Sct variables in the OGLE-III database, although more than half of them were marked as uncertain due to their low luminosity, close to the detection limit of the 1.3-m OGLE telescope. At the same time, Garg *et al.* (2010) published a list of 2300 high-amplitude  $\delta$  Sct candidates detected by the 4-m Blanco Telescope operated by the SuperMACHO project. Then, Kim *et al.* (2014) reported the discovery of 2481  $\delta$  Sct stars in the EROS-2 light curve database. These samples were supplemented with 55  $\delta$  Sct variables found by Salinas *et al.* (2018) in a field centered on the LMC globular cluster NGC 1846. All these catalogs together contain about 6600  $\delta$  Sct candidates in the LMC.

In this work, we verify these samples and significantly increase the number of known  $\delta$  Sct variables in the LMC. The remainder of this paper is organized as follows. In Section 2, we provide details about the OGLE observations and data

reduction. Section 3 outlines the procedures employed for the identification and classification of  $\delta$  Sct stars in the LMC. In Section 4, we cross-match our collection of  $\delta$  Sct variables with external catalogs of variable stars. Section 5 presents newly detected Cepheids and RR Lyr stars which were also included in the OCVS. As a by-product, we examine the contamination rates of the recently published Gaia DR3 catalogs of Cepheids (Ripepi *et al.* 2023) and RR Lyr stars (Clementini *et al.* 2023). In Section 6, we summarize the OGLE collection of  $\delta$  Sct stars in the LMC. The on-sky distribution of  $\delta$  Sct variables in the Magellanic Clouds is presented in Section 7. In Section 8, we derive the period–luminosity (PL) relations for  $\delta$  Sct stars in the LMC. The subsequent section is devoted to multimode  $\delta$  Sct pulsators. Binary systems containing  $\delta$  Sct components are discussed in Section 10. Finally, Section 11 provides a summary of our results.

## 2. Observations and Data Reduction

The OGLE observations were taken with the 1.3-meter Warsaw Telescope located at Las Campanas Observatory in Chile. The observatory is operated by the Carnegie Institution for Science. The Warsaw Telescope is equipped with a mosaic camera consisting of 32  $2k \times 4k$  CCDs with about 268 million pixels in total. The field of view of the OGLE-IV camera is 1.4 square degrees, with a pixel scale of  $0.''26$ . For our research, we utilized photometric data in two photometric bands obtained within the OGLE-IV project between March 2010 and March 2020. The majority of the observations (typically around 700 data points per object) were collected by the OGLE-IV survey using the *I*-band filter from the Cousins photometric system. Additionally, from several to over 300 (typically 120) data points per star have been secured in the *V*-band filter, closely reproducing the bandpass from the Johnson photometric system.

The OGLE-IV project regularly observes an area of 765 square degrees in the Magellanic System region, fully covering the LMC, SMC, and the Magellanic Bridge connecting both galaxies. We adopted the celestial meridian of  $2^{\text{h}}8$  as the arbitrary boundary that separates the LMC from the SMC in the sky. In the LMC region, the OGLE survey monitors the brightness of around 70 million stars with *I*-band magnitudes ranging from about 13.0 to 21.5. A detailed description of the instrumentation, photometric reductions, and astrometric calibrations of the OGLE-IV observations is provided by Udalski *et al.* (2015).

## 3. Search for $\delta$ Sct Stars

Our search for  $\delta$  Sct variables in the LMC followed procedures similar to those described in Soszyński *et al.* (2022). Firstly, the *I*-band time series of each star observed by OGLE in the LMC were passed through the period-search algorithm implemented in the FNPEAKS code<sup>†</sup>. We explored the frequency range from 0 to

---

<sup>†</sup><http://helas.astro.uni.wroc.pl/deliverables.php?lang=en&active=fnpeaks>

100 cycles per day with a resolution of  $5 \times 10^{-5}$  cycles per day. For each light curve, we measured the dominant period and then subtracted it, along with its first two harmonics, from the data. Then, we repeated the periodicity search procedure on the residuals, allowing us to measure two strongest periods for each source.

The next stage of our procedure for selecting and classifying  $\delta$  Sct stars in the LMC was based on the visual inspection of the light curves with a dominant period shorter than 0.3 d. After excluding known eclipsing variables and RR Lyr stars, we examined the  $I$ - and  $V$ -band light curves of over 100 thousand stars with the largest signal-to-noise ratios of their periods. Although the OGLE  $V$ -band light curves consist of a smaller number of data points compared to the  $I$ -band time series, this is compensated by lower noise in the  $V$  filter for most  $\delta$  Sct variables. Based on the characteristic shapes of the light curves, we selected an initial sample of candidate  $\delta$  Sct stars. Furthermore, we identified a number of double-mode pulsators based on their high signal-to-noise secondary periods and period ratios in the range of 0.75 to 0.81 (see Section 9).

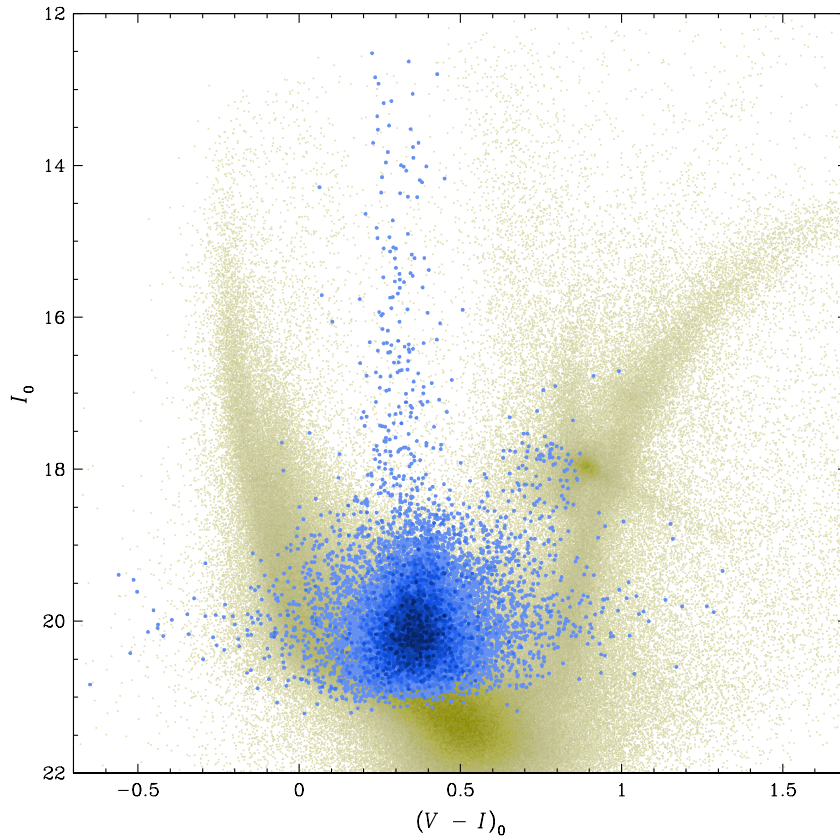


Fig. 1.  $(V - I)_0$  vs.  $I_0$  color-magnitude diagram for  $\delta$  Sct stars in the LMC (blue points). The background yellow points show stars from the field LMC519. Darker colors indicate areas of higher density of the points. The colors and magnitudes have been corrected for interstellar extinction using the reddening maps by Skowron *et al.* (2021).

In the last stage, we verified our candidates by checking their positions on the color–magnitude and PL diagrams. Fig. 1 shows the color–magnitude diagram for  $\delta$  Sct stars in the LMC. The  $I$ -band magnitudes and  $(V - I)$  color index have been corrected for interstellar extinction using the high-resolution reddening maps by Skowron *et al.* (2021). During the selection process, most of the sources with a dereddened color index outside the range  $0.1 < (V - I)_0 < 0.7$  mag (corresponding to the instability strip for  $\delta$  Sct variables) have been removed from our initial list. However, approximately 5% of the stars in the final version of our collection have colors outside this range because we considered that they may be genuine  $\delta$  Sct pulsators blended with other stars. The result of our selection procedure was an initial list of approximately 14 000  $\delta$  Sct stars in the direction of the LMC.

#### 4. Comparison with the Literature

In order to assess the completeness and contamination rate of the OGLE collection of  $\delta$  Sct stars in the LMC, we cross-matched it with several lists of variable stars, including the catalogs published by the OGLE-III (Poleski *et al.* 2010), SuperMACHO (Garg *et al.* 2010), and EROS-2 (Kim *et al.* 2014) projects, the International Variable Star Index (VSX, Watson *et al.* 2006), and the Gaia DR3 catalog of main-sequence pulsators (Gaia Collaboration *et al.* 2023). We carefully examined the light curves of  $\delta$  Sct candidates that were not present in the initial version of our collection and supplemented it with over 1000 objects that we identified as genuine  $\delta$  Sct pulsators. The final OGLE collection contains 4712 stars that were identified as  $\delta$  Sct variables in previously released catalogs. This means that 10 544 objects in our sample (69%) are new discoveries. Below, we present detailed results of the comparison between the OGLE collection and other catalogs of  $\delta$  Sct stars in the LMC.

Our collection shares 2309 sources with the OGLE-III catalog of 2788  $\delta$  Sct candidates in the LMC (Poleski *et al.* 2010). For the remaining 479 objects (representing about 17% of the OGLE-III catalog), we were unable to confirm the classification provided by Poleski *et al.* (2010). Several of these stars have been reclassified as classical Cepheids or RR Lyr variables, several dozen other sources turned out to be eclipsing or ellipsoidal variables, but the majority of the rejected stars have an unknown classification. While it is possible that some of these objects are true  $\delta$  Sct stars, we decided to exclude them from the OCVS in order to maintain the purity of our sample. It is worth noting that the vast majority of the rejected stars were marked as uncertain in the OGLE-III catalog.

The SuperMACHO catalog of high-amplitude  $\delta$  Sct stars in the LMC (Garg *et al.* 2010) contains 2300 objects<sup>‡</sup>. The SuperMACHO project (Rest *et al.* 2005) was an optical survey of the LMC conducted with the 4-m Blanco telescope at

---

<sup>‡</sup>Garg *et al.* (2010) reported the discovery of 2323 candidates for  $\delta$  Sct variables, however, 23 of them have been duplicated in the SuperMACHO catalog.

the Cerro Tololo InterAmerican Observatory in Chile. The SuperMACHO photometry is deeper than the OGLE photometry obtained with the 1.3-meter Warsaw telescope, which is the main reason why 308  $\delta$  Sct stars discovered by Garg *et al.* (2010) are missing in our collection. In turn, we confirm the classification of 1992 brighter variables, which indicates a high level of purity of the SuperMACHO catalog.

The EROS-2 catalog (Kim *et al.* 2014) comprises 117 234 automatically classified variable stars in the LMC, of which 2481 are categorized as  $\delta$  Sct candidates. It is worth noting that the list published by Kim *et al.* (2014) contains in total 150 115 candidates for variable stars, however objects fainter than  $B_E = 20$  mag and those with low signal-to-noise ratios ( $S/N < 20$ ) of their periods were considered false positives and thus excluded from the official EROS-2 catalog. Following this approach, we also excluded these faint and low-signal-to-noise EROS-2 sources from our cross-match. Our collection includes 1376 out of 2481 objects classified by Kim *et al.* (2014) as  $\delta$  Sct stars, which represents about 56% of the EROS-2 sample. Among the missing stars, we found, over 300 eclipsing binary systems, more than 50 RR Lyr variables, some irregular variables, and constant stars.

Comparison of our  $\delta$  Sct sample with the VSX catalog (Watson *et al.* 2006) revealed 30 common objects, all of which are brighter than  $I = 16.5$  mag, indicating they are foreground stars. The vast majority of these variables were discovered by the All-Sky Automated Survey for Supernovae (ASAS-SN, Jayasinghe *et al.* 2019, Christy *et al.* 2023). In the catalog of main-sequence pulsators published as part of the Gaia DR3 (Gaia Collaboration *et al.* 2023), we identified 49  $\delta$  Sct stars that overlap with our sample. All of these variables also belong to the halo of the Milky Way. Additionally, our collection contains 71 variables classified in the Gaia DR3 catalog as RR Lyr stars, eclipsing binaries, or short-timescale variables.

## 5. New Cepheids and RR Lyr Stars. Comparison to the Gaia DR3 Catalog

Our search for  $\delta$  Sct variables in the Magellanic System and the cross-match of the OGLE databases with the Gaia DR3 catalog of variable stars (Clementini *et al.* 2023, Ripepi *et al.* 2023) allowed us to expand the OGLE collection of Cepheids and RR Lyr stars (Soszyński *et al.* 2015a, 2016, 2017, 2019). Population I  $\delta$  Sct stars and classical Cepheids form a continuous distribution, therefore we adopted a boundary pulsation period that separates these two types of variables. As it was reasoned in Soszyński *et al.* (2022), we applied a maximum period of 0.3 d for the fundamental mode and 0.23 d for the first-overtone mode in  $\delta$  Sct stars. Population I pulsators with longer periods are categorized as classical Cepheids in the OCVS.

The adoption of these strict criteria resulted in the reclassification of several pulsating stars already present in the OCVS, although this change is purely formal. Two multimode variables with the first-overtone periods shorter than 0.23 d were

moved from the list of classical Cepheids to the collection of  $\delta$  Sct stars. On the other hand, four stars classified by Poleski *et al.* (2010) as  $\delta$  Sct stars have pulsation periods that, according to our new criteria, place them among Cepheids, so they were included in the OGLE collection of classical Cepheids in the LMC (Soszyński *et al.* 2015ab). In addition, the classification of six pulsators with periods above 0.2 d has been changed from  $\delta$  Sct to first-overtone RR Lyr (RRc) stars. In these cases, we mainly relied on their position in the PL diagram, as they fall on the relation for RRc stars, *i.e.*, below the PL sequence for delta Scuti stars. Table 1 contains all the reclassified classical pulsators in the LMC that have been moved between the OGLE catalogs of Cepheids, RR Lyr stars, and  $\delta$  Sct stars.

Table 1

Reclassified variable stars from the OCVS

Old identifier	New identifier	New classification	Subtype
OGLE-LMC-CEP-3367	OGLE-LMC-DSCT-07569	$\delta$ Sct star	1O/2O
OGLE-LMC-CEP-3374	OGLE-LMC-DSCT-11916	$\delta$ Sct star	1O/2O/3O
OGLE-LMC-DSCT-0394	OGLE-LMC-RRLYR-41407	RR Lyr star	RRc
OGLE-LMC-DSCT-0434	OGLE-LMC-CEP-4716	Classical Cepheid	1O
OGLE-LMC-DSCT-0662	OGLE-LMC-CEP-4717	Classical Cepheid	F/1O
OGLE-LMC-DSCT-0765	OGLE-LMC-RRLYR-41427	RR Lyr star	RRc
OGLE-LMC-DSCT-0927	OGLE-LMC-CEP-4718	Classical Cepheid	F/1O/2O
OGLE-LMC-DSCT-1305	OGLE-LMC-CEP-4720	Classical Cepheid	1O
OGLE-LMC-DSCT-1428	OGLE-LMC-RRLYR-41452	RR Lyr star	RRc
OGLE-LMC-DSCT-1709	OGLE-LMC-RRLYR-41461	RR Lyr star	RRc
OGLE-LMC-DSCT-1955	OGLE-LMC-RRLYR-41467	RR Lyr star	RRc
OGLE-LMC-DSCT-2716	OGLE-LMC-RRLYR-41514	RR Lyr star	RRc

Our collection of variable stars has also been enriched with additional Cepheids and RR Lyr stars identified as by-products of the search for  $\delta$  Sct pulsators, as well as through cross-matching with the Gaia DR3 catalog of variable stars (Clementini *et al.* 2023, Ripepi *et al.* 2023). The number of classical Cepheids in the LMC increased by five objects (including a very rare case of a double-mode pulsator with the second- and third-overtone modes simultaneously excited), type II Cepheids by one, anomalous Cepheids by two, and RR Lyr stars by 355 previously overlooked variables. These stars were omitted in the earlier editions of the OCVS due to a small number of measurement points in the OGLE light curves, or noisy photometry, or symmetric light curves, or pulsation periods close to 1/2 d, which led to an erroneous measurement of the period due to a daily alias. This update resulted in an increase of the OGLE sample of Cepheids in the LMC by less than 0.2%, while the list of RR Lyr stars grew by less than 1%, confirming the high completeness of the OCVS in the Magellanic Clouds.

We also utilized the Gaia DR3 catalog to validate the completeness of the OGLE collection of classical pulsating stars in the Galactic bulge and disk (Udalski *et al.* 2018, Pietrukowicz *et al.* 2020, Soszyński *et al.* 2020, 2021). Firstly, we cross-matched the Gaia catalog with the OCVS. Then, we extracted and carefully examined the OGLE light curves of candidate pulsators that were not previously included in our collection. As a result, the OCVS was supplemented with 108 Galactic Cepheids of all types (representing 2.9% of the previously published sample), 1848 RR Lyr stars (2.4%), and 94  $\delta$  Sct stars (0.4%).

As a by-product of our analysis, we examined the contamination rates of the Gaia DR3 catalogs of Cepheids and RR Lyr stars. The final version of the Gaia catalog contains 15 006 candidates for classical, type II, and anomalous Cepheids in the Milky Way, Magellanic Clouds, M31, and M33 (Ripepi *et al.* 2023). The OGLE photometric databases provide time-series data for 12 139 of these stars. We confirm that the vast majority of them, over 97%, are indeed Cepheids. Among the remaining stars, we identified more than 50 eclipsing and ellipsoidal variables, over 50 objects were classified by the OGLE team as RR Lyr or  $\delta$  Sct stars, we also identified some long-period variables, spotted variables, and other types of variable stars. Furthermore, the detailed division into classical and type II Cepheids agrees well in the Gaia DR3 catalog and OCVS. The only exception are anomalous Cepheids, as over 40% of the stars categorized as anomalous Cepheids in the Gaia DR3 catalog have a different classification in the OGLE collection.

The Gaia DR3 catalog contains 270 905 candidates for RR Lyr stars (Clementini *et al.* 2023), out of which 148 401 are observed by the OGLE survey. We confirmed the Gaia classification for 104 346 (approximately 70%) of these stars. Among the remaining  $\approx 44\,000$  objects, we discovered around 300 eclipsing variables and some other types of variable stars. However, the vast majority of the Gaia RR Lyr candidates in this group show no periodic variability at all. We conducted a visual inspection of both the OGLE *I*-band and Gaia *G*-band light curves of these misclassified stars and noticed that most of them are faint ( $G > 20$  mag), close to the detection limit of the Gaia telescope. The Gaia time-series photometry for these objects is usually quite noisy, and the periods provided in the Gaia DR3 catalog appear to be random measurements fitted to outlier data points in the light curves. Further analysis revealed a pronounced correlation between the contamination from non-RR Lyr sources and the brightness of stars in the Gaia DR3 catalog. The contamination rate equals approximately 1% for objects brighter than  $G = 19$  mag, it increases to 21% for sources with mean *G*-band magnitudes ranging from 19 to 20 mag, and escalates to nearly 90% for stars fainter than  $G = 20$  mag.

## 6. The OGLE Collection of $\delta$ Sct Stars in the LMC

The definitive version of our collection comprises 15 256  $\delta$  Sct variables found in the OGLE fields toward the LMC. Approximately 15 000 of these stars belong to the LMC, while the remaining objects are part of the Milky Way’s halo. The major-

ity of  $\delta$  Sct stars in our sample exhibit radial pulsation in either the fundamental or first-overtone mode, as indicated by relatively large amplitudes of their light curves and position in the PL diagram (see Section 8). However, we refrain from providing the presumed pulsation modes of our variables due to the challenges associated with their identification in specific cases. Instead, we have divided our  $\delta$  Sct sample into single mode and multimode pulsators. The latter category encompasses 639 stars (about 4% of the entire catalog) that feature substantial amplitudes of their secondary or tertiary pulsation modes.

The list of our  $\delta$  Sct stars together with their basic parameters (equatorial coordinates, intensity-averaged mean magnitudes in the  $I$  and  $V$  bands, up to three pulsation periods, amplitudes, epochs of the maximum light, and Fourier coefficients), as well as OGLE-IV time-series photometry, can be accessed through the OGLE Internet Archive:

<https://ogle.astrouw.edu.pl>  $\rightarrow$  *OGLE Collection of Variable Stars*  
<https://www.astrouw.edu.pl/ogle/ogle4/OCVS/lmc/dsct/>

For the  $\delta$  Sct candidates published in the OGLE-III catalog of variable stars (Poleski *et al.* 2010), we maintained their designations in the format of OGLE-LMC-DSCT-NNNNN (where NNNNN represents a consecutive number), while only extending the number of digits in the designation from four to five. The newly added  $\delta$  Sct stars have been organized by their right ascension and given designations from OGLE-LMC-DSCT-02789 to OGLE-LMC-DSCT-15735.

The pulsation periods, along with their uncertainties, were computed using the TATRY code (Schwarzenberg-Czerny 1996) based on the OGLE-IV light curves obtained between 2010 and 2020. To expand the temporal coverage of the photometric data from 10 to even over 20 years, the OGLE-IV light curves can be merged with the OGLE-III and OGLE-II time series provided by Poleski *et al.* (2010). However, it is crucial to consider the possibility of zero-point offsets between these datasets for individual stars.

Fig. 2 illustrates the distributions of pulsation periods (upper panel), apparent  $I$ -band mean magnitudes (middle panel), and  $I$ -band peak-to-peak amplitudes (lower panel) of  $\delta$  Sct stars in the LMC and SMC (Soszyński *et al.* 2022). The shapes of these histograms reflect both the intrinsic characteristics of the  $\delta$  Sct population in the Magellanic Clouds and the limitations of the OGLE photometry. The faintest objects in our collection of  $\delta$  Sct stars in the LMC have mean brightness of about  $I = 21.3$  mag, but the number of variables in our sample starts to decline beyond a luminosity of  $I = 20.5$  mag. It can be attributed to the pronounced correlation between the amplitude detection limits and the observed magnitudes of pulsating stars. For example, for variables with the mean brightness around  $I = 20$  mag, the smallest detectable amplitudes are approximately 0.1 mag, while for stars with  $I = 21$  mag, the amplitude detection limit increases to about 0.2 mag.

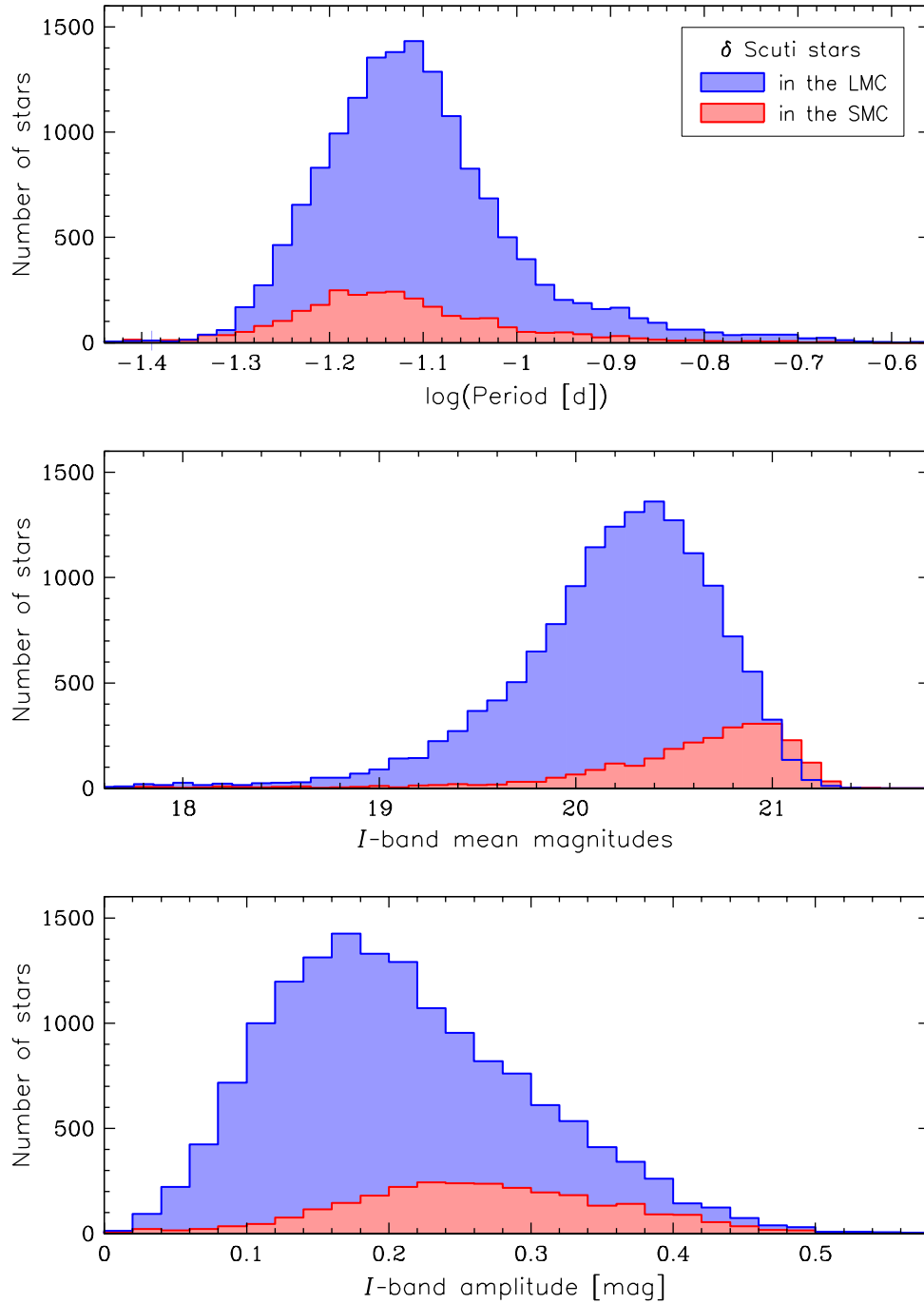


Fig. 2. Distributions of dominant pulsation periods (*upper panel*),  $I$ -band mean magnitudes (*middle panel*), and  $I$ -band peak-to-peak amplitudes (*lower panel*) of 15 256  $\delta$  Sct stars in the LMC (blue histograms) and 2810  $\delta$  Sct stars in the SMC (red histograms).

Keeping in mind these luminosity and amplitude detection limits of the OGLE survey, we evaluated the completeness of our collection by considering stars that were identified twice within overlapping regions of adjacent fields. In the final iteration of our catalog, each  $\delta$  Sct pulsator is uniquely represented by a single entry from the OGLE database, typically favoring the one with a greater number of data points in its light curve. We retrospectively checked that 1162  $\delta$  Sct stars in our collection are located in the overlapping parts of neighboring OGLE-IV fields, implying that we could potentially detect 2324 objects from this group. In practice, we independently confirmed the classification of both components in 624 such pairs, whereas in 538 cases, only one component of the pair was identified. Consequently, this leads to the catalog completeness level of approximately 70%. Once again, we emphasize that this value applies to  $\delta$  Sct stars in the LMC, whose luminosities and amplitudes are sufficiently large to be detectable with the OGLE photometry.

## 7. On-sky Map

The upper panel of Fig. 3 displays the on-sky distribution of about 17 600  $\delta$  Sct pulsators in the LMC and SMC (Soszyński *et al.* 2022), while the lower panel shows the positions of approximately 400 SX Phe variables likely belonging to the Milky Way’s halo. The latter group consists of stars that are at least 1.5 mag brighter than the average PL relation fulfilled by  $\delta$  Sct variables in the LMC or SMC, respectively.

The spatial distributions of different stellar populations provide valuable information about their history. For example, the ancient population of RR Lyr pulsators (Soszyński *et al.* 2016) in the LMC exhibits a structure that can be approximated by a triaxial ellipsoid without any additional substructures (*e.g.*, Jacyszyn-Dobrzyniecka *et al.* 2017). Conversely, classical Cepheids, which are stars younger than 300 million years, tend to concentrate in the LMC bar and spiral arms (*e.g.*, Soszyński *et al.* 2015a, Jacyszyn-Dobrzyniecka *et al.* 2016).  $\delta$  Sct stars also follow the bar and spiral arms of the LMC (Fig. 3), although this pattern is not as distinct as in the case of classical Cepheids, indicating that the majority of our  $\delta$  Sct sample consists of intermediate-age stars.

In the region of the LMC bar, the maximum surface density of  $\delta$  Sct stars from our catalog exceeds 600 objects per square degree. The surface density drops almost to zero at a distance of 5 degrees from the center of the LMC (toward the South) or 9 degrees (toward the North), while the distribution of RR Lyr stars extends to much larger distances (*e.g.*, Soszyński *et al.* 2016). This indicates that our collection of  $\delta$  Sct pulsators in the Magellanic Clouds is primarily comprised of Population I stars, while the majority of Population II SX Phe variables in the LMC and SMC are too faint to be detected in the OGLE frames. Of course, this statement does not apply to foreground  $\delta$  Sct stars in the halo of the Milky Way, which by definition belong to Population II.

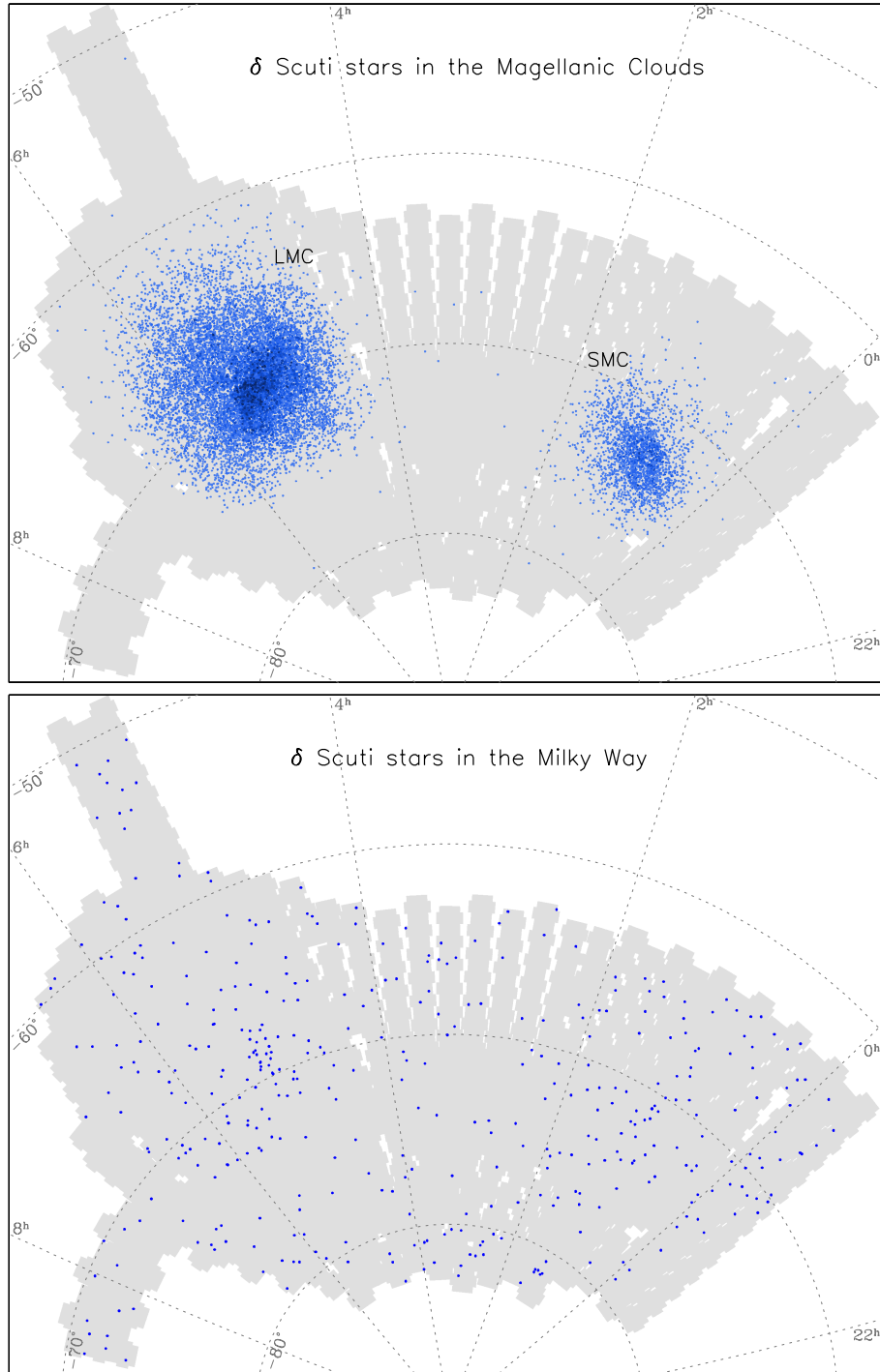


Fig. 3. On-sky distribution of  $\delta$  Sct stars in the direction of the Magellanic Clouds. *Upper panel* displays the positions of more than 17 600 probable members of the LMC and SMC, while *lower panel* shows  $\delta$  Sct variables that are likely part of the Milky Way halo. The gray area represents the OGLE footprint in the Magellanic System region.

## 8. Period–Luminosity Relations

The investigation of the PL relations followed by  $\delta$  Sct pulsators is one of the most important applications of our collection. Many empirical calibrations of the PL relations for  $\delta$  Scuti stars have been reported in the literature (*e.g.*, Nemec *et al.* 1994, Cohen and Sarajedini 2012, Ziaali *et al.* 2019, Jayasinghe *et al.* 2020, Barac *et al.* 2022, Ngeow *et al.* 2023), but most were based on nearby variables with well-determined parallaxes or SX Phe stars identified in the Galactic globular clusters, the distances to which were known from other standard candles, for example RR Lyr stars.

The LMC has many advantages in the context of studying the distribution of various classes of pulsating stars in the PL plane. The close proximity, favorable orientation, and low average reddening toward this galaxy offers a unique opportunity for conducting in-depth analyses of its stellar component. The LMC hosts large and diverse populations of variable stars, including some of the largest known samples of Cepheids, RR Lyr stars, and long-period variables. Moreover, the distance to the LMC is currently known to an unprecedented accuracy of 1% (Pietrzyński *et al.* 2019).

Previous efforts to measure the PL relationships for  $\delta$  Sct stars in the LMC (McNamara *et al.* 2007, Garg *et al.* 2010, Poleski *et al.* 2010, McNamara 2011) relied on small or biased samples of variables. Recently, Martínez-Vázquez *et al.* (2022) gathered data for approximately 4000 extragalactic  $\delta$  Sct variables (primarily from the LMC) and investigated their distribution in the PL plane. They concluded that extragalactic  $\delta$  Sct stars exhibit a single PL relationship with a notable change in slope occurring at a period of around 0.09 d.

The OGLE collection of about 15 000  $\delta$  Sct stars in the LMC enables us to verify these results. In Fig. 4, we present four versions of the extinction-corrected *I*-band PL diagram for our sample. In the upper left panel (a), different colors of points denote different amplitudes of brightness variations. In this diagram, two linear PL relationships can be discerned, with variables of larger amplitudes prevailing along the lower ridge. Due to the significant dispersion of points around these relationships, in panel b of Fig. 4, we provide a density map of the points on this diagram. There is no doubt that  $\delta$  Sct stars in the LMC follow two PL relationships without apparent changes in slope. This contradicts the findings of Martínez-Vázquez *et al.* (2022), who reported a single segmented PL relation, which probably was an illusion resulting from incompleteness of the prior catalogs of extragalactic  $\delta$  Sct stars.

The identification of the pulsation modes corresponding to both PL ridges can be achieved by plotting double-mode  $\delta$  Sct pulsators with period ratios in the range of 0.755–0.785, *i.e.*, corresponding to the simultaneous oscillations in the fundamental and first-overtone modes (see Section 9). The color symbols in panel c

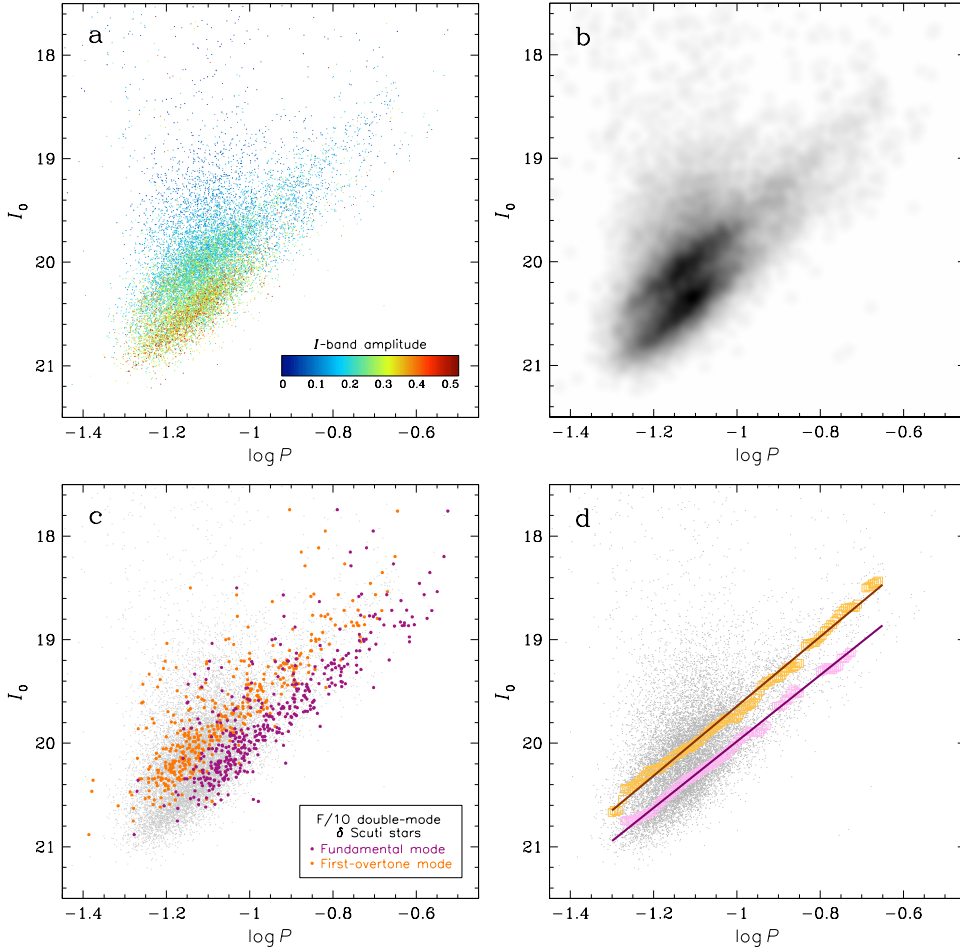


Fig. 4. Extinction-corrected  $I$ -band PL diagram for  $\delta$  Sct stars in the LMC. *Panel a:* the colors of the points represent peak-to-peak amplitudes of the  $I$ -band light curves, as indicated by the scale in the bottom right corner. *Panel b:* density map of the points in the PL diagram. *Panel c:* PL diagram for double-mode  $\delta$  Sct stars pulsating in the fundamental (purple points) and first-overtone (orange points) modes. Background gray dots represent single-mode  $\delta$  Sct stars. *Panel d:* linear least-square fits to the fundamental-mode (purple line) and first-overtone (orange line) PL relations of  $\delta$  Sct stars in the LMC. Yellow and pink squares indicate local maxima of the magnitude distribution.

of Fig. 4 unambiguously indicate that the lower ridge is populated by  $\delta$  Sct variables pulsating in the fundamental mode, while the upper ridge is composed of the first-overtone pulsators.

In order to fit the most precise regression lines to both relations in the  $I$ -band, we constructed histograms of brightness for consecutive period bins (each with a bin size of 0.05 in  $\log P$ , moved by  $\Delta \log P = 0.005$ ). Then, we found two local maxima (corresponding to the fundamental-mode and the first-overtone ridges) of the magnitude distributions for each period bin. Any unreliable determinations of the maxima (*e.g.*, due to a limited number of stars within a bin) were excluded. Finally, we performed linear least-square fits to the obtained points. The result

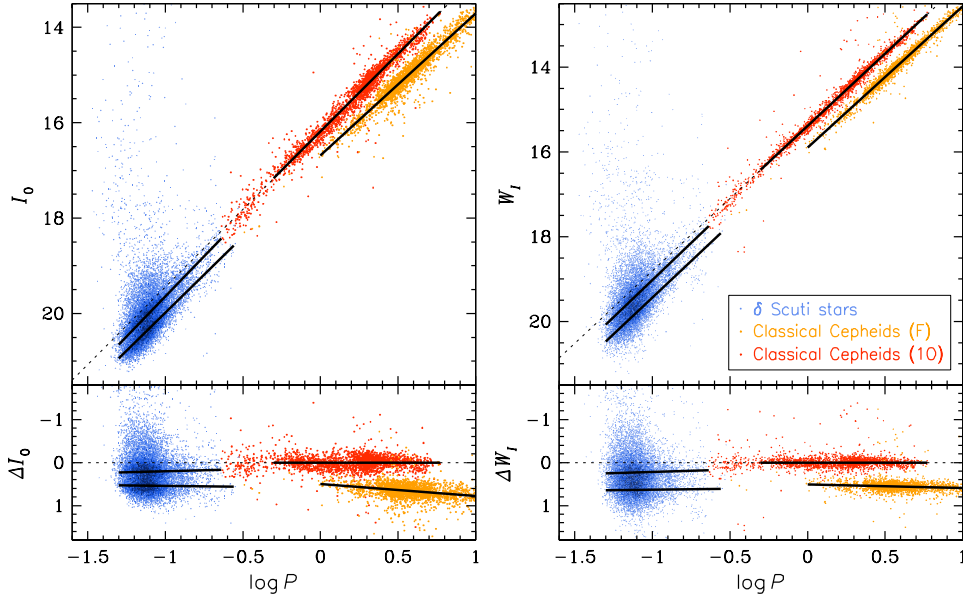


Fig. 5. PL (left panels) and PW (right panels) diagrams for  $\delta$  Sct stars and classical Cepheids in the LMC. Blue, orange, and red points mark  $\delta$  Sct variables, fundamental-mode classical Cepheids, and first-overtone classical Cepheids, respectively. Solid lines represent fits to the PL and PW relations. Dashed lines are the extensions of the PL and PW relationships for first-overtone Cepheids with periods longer than 0.5 d. Lower panels show the residuals with respect to the fit applied to the first-overtone classical Cepheids with periods longer than 0.5 d.

of our procedure is shown in panel d of Fig. 4 and summarized in Table 2. The same method was used to fit the  $V$ -band PL relations as well as the period– $W_I$  (PW) relations, where  $W_I$  is an extinction-insensitive Wesenheit index, defined as  $W_I = I - 1.55(V - I)$ .

The dispersion of points around the average PL and PW relations is significant ( $\sigma \approx 0.2$  mag), which may stem from measurement errors of the photometry, blending by unresolved sources, the geometry of the LMC, differential interstellar extinction, as well as the diversity of stellar populations present in our sample. In particular, it is recognized that SX Phe stars are systematically underluminous relative to Population I  $\delta$  Sct pulsators (McNamara *et al.* 2007).

The PL and PW relations for  $\delta$  Sct stars (Table 2) are distinctly steeper than the relations for classical Cepheids (Soszyński *et al.* 2015a) pulsating in the same modes. In Fig. 5, we display the  $I$ -band PL diagram (left panel) and PW diagram (right panel) for  $\delta$  Sct stars and classical Cepheids in the LMC. The first-overtone variables lay along a continuous ridge in both diagrams, whereas the fundamental-mode pulsators demonstrate a discontinuity within the period range of approximately 0.3–1.0 d, except for several multimode Cepheids with the fundamental-mode periods falling within this range.

The lower panels of Fig. 5 show the residuals with respect to the linear fit applied to the first-overtone classical Cepheids with periods longer than 0.5 d. The

Table 2

Period–Luminosity and Period–Wesenheit Relations for  $\delta$  Sct stars in the LMC

Mode of pulsation	$\alpha$	$\beta$
	$I_0 = \alpha \log P + \beta$	
Fundamental	$-3.203 \pm 0.024$	$16.778 \pm 0.025$
First-overtone	$-3.353 \pm 0.027$	$16.290 \pm 0.026$
	$V_0 = \alpha \log P + \beta$	
Fundamental	$-3.048 \pm 0.025$	$17.341 \pm 0.027$
First-overtone	$-3.154 \pm 0.028$	$16.822 \pm 0.029$
	$W_I = \alpha \log P + \beta$	
Fundamental	$-3.449 \pm 0.026$	$15.986 \pm 0.028$
First-overtone	$-3.522 \pm 0.029$	$15.501 \pm 0.030$

dashed line, which is an extension of this relation, lies above the majority of the  $\delta$  Sct stars, confirming the non-linear nature of the continuous PL and PW relationships for first-overtone Cepheids and  $\delta$  Sct variables. Moreover, most short-period overtone Cepheids also reside below this dashed line, indicating that the change in the slope of the PL and PW relations occurs at period of about 0.5 d ( $\log P \approx 0.3$ ). This break in the PL relation for first-overtone classical Cepheids was first noticed by Soszyński *et al.* (2008). Recently, Ripepi *et al.* (2022) confirmed the non-linearity of the first-overtone PL and PW relations in the near-infrared bands, pinpointing the break point at  $P_{IO} = 0.58 \pm 0.1$  d.

## 9. Multimode $\delta$ Sct Stars

Stars that pulsate in multiple modes are attractive targets for asteroseismological research. Within the general population of  $\delta$  Sct stars, most objects are low-amplitude variables with a number of non-radial modes simultaneously excited (Breger 2000). However, due to the limitations of the OGLE photometry, the proportions of low- and high-amplitude variables are inverted in our collection. The predominant portion of LMC  $\delta$  Sct stars within our sample demonstrates high-amplitude oscillations in the fundamental or first-overtone modes.

In our collection, we provide up to three pulsation periods per star. However, for the majority of variables, only a dominant period could be reliably measured. Secondary or tertiary periods were identified only when their amplitudes exceeded the detection thresholds of the OGLE photometry. As a result, the final version of our catalog includes 621 double-mode and only 18 triple-mode  $\delta$  Sct variables.

Fig. 6 shows the Petersen diagram (a plot of the ratio between two periods against the logarithm of the longer one) for multimode  $\delta$  Sct stars, classical Cepheids (Soszyński *et al.* 2015b), and RR Lyr variables (Soszyński *et al.* 2016) in the

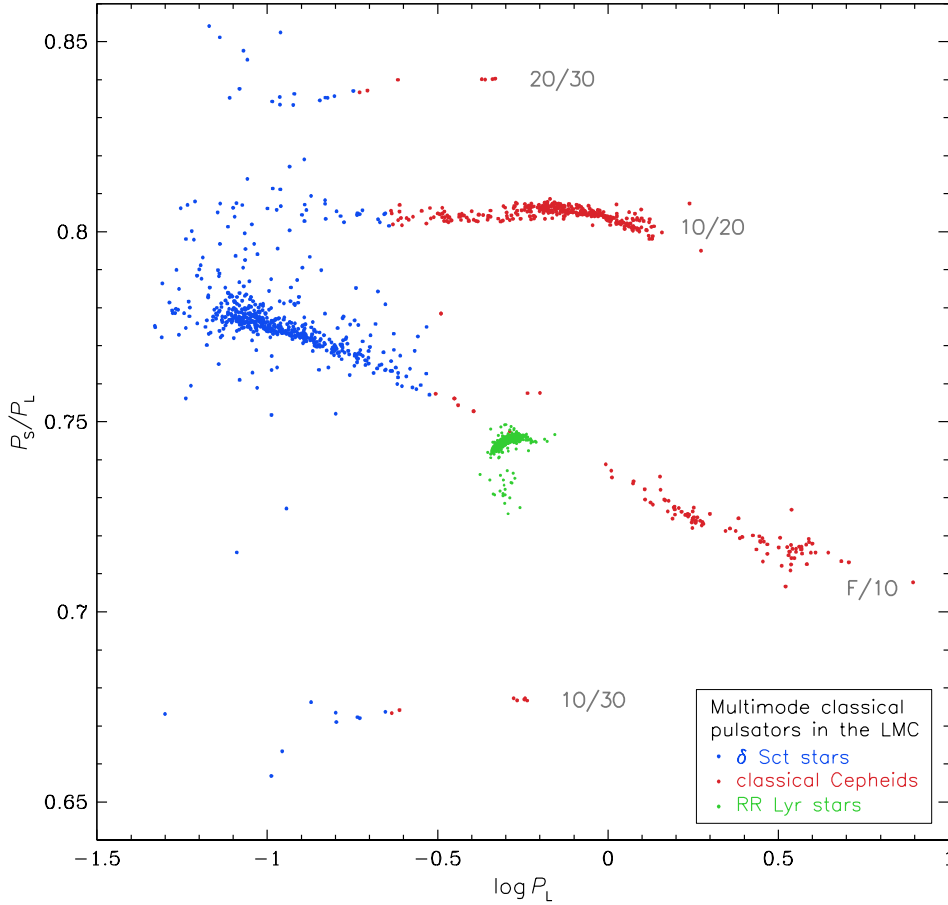


Fig. 6. Petersen diagram for multimode  $\delta$  Sct stars (blue points), classical Cepheids (red points), and RR Lyr stars (green points) in the LMC.

LMC. As expected, we predominantly detected stars oscillating in two or three low-order radial modes, particularly in the fundamental and first-overtone modes (F/1O). Roughly two-thirds of all multimode  $\delta$  Sct pulsators in our sample have these two modes excited. Additionally, our dataset includes about 50 double- and triple-mode  $\delta$  Sct stars simultaneously pulsating in the first, second, or third overtones (in various configurations), and about 80 variables exhibiting secondary periods very close to the primary ones. The latter phenomenon may indicate the presence of the non-radial modes.

Fig. 6 vividly illustrates the continuity between  $\delta$  Sct stars and classical Cepheids in the Petersen diagram. The choice of pulsation periods that distinguishes both classes of variable stars is a matter of convention. In the OCVS, we adopted  $P_F = 0.3$  d for the fundamental mode,  $P_{1O} = 0.23$  d for the first-overtone, and  $P_{2O} = 0.185$  d for the second overtone.

The Petersen diagram is a powerful tool to constrain stellar parameters such as masses or metallicities of multimode pulsators (*e.g.*, Petersen and Christensen-

Dalgaard 1996, Poretti *et al.* 2005, Netzel *et al.* 2022). Fig. 7 shows a zoom-in of the Petersen diagram focusing on the region occupied by F/10  $\delta$  Sct stars in the Milky Way (Soszyński *et al.* 2021), SMC (Soszyński *et al.* 2022), and LMC (this work).

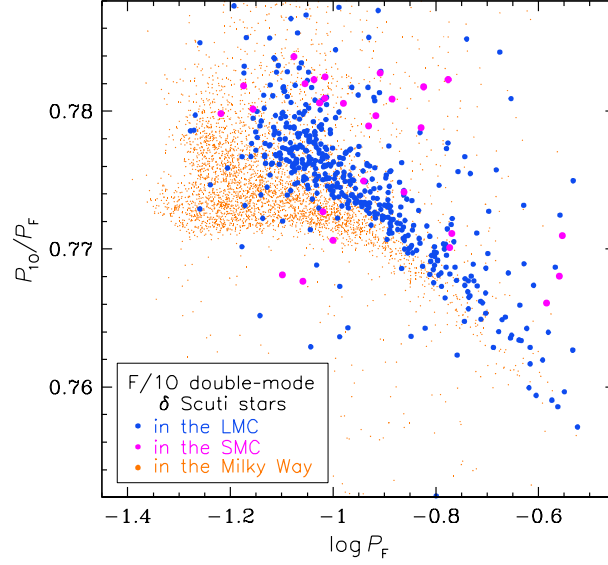


Fig. 7. Petersen diagram for F/10 double-mode  $\delta$  Sct stars in the LMC (blue points), SMC (magenta points), and Milky Way (orange points).

The Galactic double-mode pulsators exhibit a characteristic splitting of the period–period ratio sequence at the short-period end. This reflects the division of  $\delta$  Sct variables into the Population I stars ( $P_{10}/P_F \approx 0.773$ ) and SX Phe stars ( $P_{10}/P_F \approx 0.778$ , Breger 2000). Double-mode pulsators with such short periods are not present in the OGLE collection of  $\delta$  Sct stars in the Magellanic Clouds due to a selection bias. These stars are too faint to be identified through OGLE photometry. Nonetheless, it is evident that the period–period ratio sequence for  $\delta$  Sct stars in the LMC is situated above the sequence for Galactic stars, and even further above lie the SMC pulsators. Double-mode F/10 classical Cepheids in the Milky Way, LMC, and SMC exhibit analogous behavior (*e.g.*, Udalski *et al.* 2018), which can be attributed to the different metallicities among these three galaxies.

## 10. $\delta$ Sct Stars in Binary Systems

Eclipsing binary systems offer a unique opportunity to accurately measure the physical parameters of the stellar components, such as masses, radii, luminosities, and temperatures. As a result, binaries comprising pulsating stars serve as excellent testbeds for asteroseismology and stellar evolution theory.  $\delta$  Sct variables within binary systems are not infrequently encountered entities. According to the updated

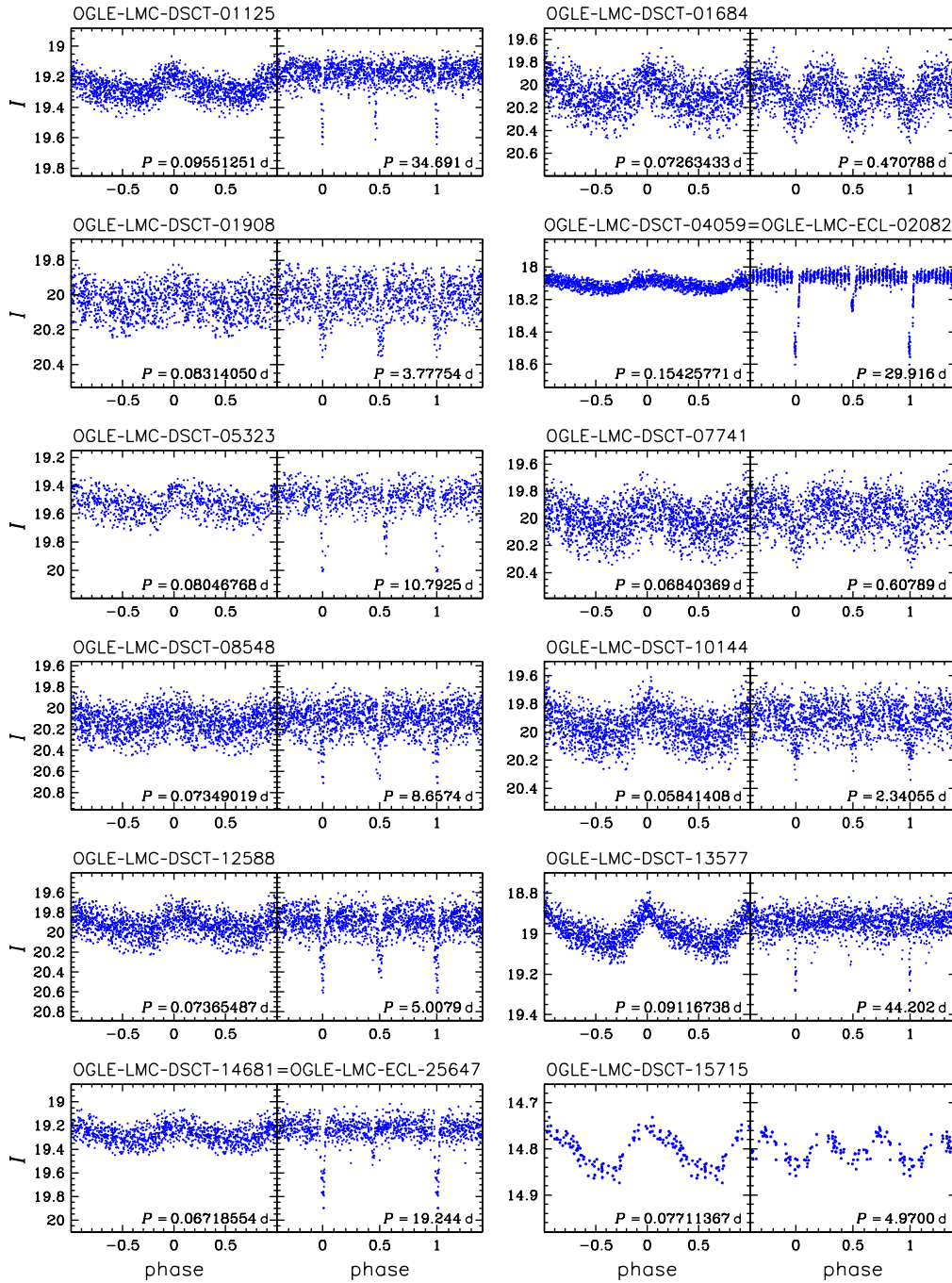


Fig. 8. Disentangled  $I$ -band light curves of  $\delta$  Sct stars showing additional eclipsing or ellipsoidal modulation. In each pair, *left panel* displays the pulsation light curve, while *right panel* shows the eclipsing/ellipsoidal light curve after subtracting the pulsation component.

version of the Liakos and Niarchos (2017) catalog<sup>§</sup>, a total of 367 binaries with a  $\delta$  Sct component have been known so far, including 34 such objects identified by the OGLE team (Pietrukowicz *et al.* 2020, Soszyński *et al.* 2021). However, all of these systems are situated within the Milky Way.

While searching for potential secondary periods in the light curves of  $\delta$  Sct stars in the LMC, we discovered 12 objects demonstrating additional variability caused by binarity, *i.e.*, eclipses or ellipsoidal variations. The details of these stars, including their coordinates, mean magnitudes, pulsation and orbital periods, are provided in Table 3. Fig. 8 displays their disentangled pulsating and eclipsing/ellipsoidal light curves. To our best knowledge, these stars are the first known extragalactic candidates for binary systems containing  $\delta$  Sct components. The spectroscopic examination of these objects will be challenging due to their low apparent luminosity. Nevertheless, the long-term OGLE photometry could be useful in studying *e.g.*, the stability of their orbital periods or the apsidal motion in the systems featuring eccentric orbits.

Table 3

$\delta$  Sct stars with additional eclipsing or ellipsoidal modulation

Identifier	R.A. [J2000.0]	Dec. [J2000.0]	$\langle I \rangle$ [mag]	$\langle V \rangle$ [mag]	$P_{\text{puls}}$ [d]	$P_{\text{orb}}$ [d]
OGLE-LMC-DSCT-01125	05 <sup>h</sup> 15 <sup>m</sup> 35 <sup>s</sup> .13	−68°36′55″.3	19.162	19.664	0.09551251	34.691
OGLE-LMC-DSCT-01684	05 <sup>h</sup> 26 <sup>m</sup> 57 <sup>s</sup> .48	−70°05′24″.1	20.053	20.447	0.07263433	0.47079
OGLE-LMC-DSCT-01908	05 <sup>h</sup> 30 <sup>m</sup> 09 <sup>s</sup> .29	−69°02′46″.1	20.004	20.366	0.08314050	3.77754
OGLE-LMC-DSCT-04059	04 <sup>h</sup> 52 <sup>m</sup> 56 <sup>s</sup> .49	−69°32′20″.0	18.057	18.905	0.15425771	29.916
OGLE-LMC-DSCT-05323	05 <sup>h</sup> 02 <sup>m</sup> 24 <sup>s</sup> .90	−67°09′49″.1	19.480	20.094	0.08046768	10.7925
OGLE-LMC-DSCT-07741	05 <sup>h</sup> 16 <sup>m</sup> 46 <sup>s</sup> .31	−69°11′19″.5	19.939	20.250	0.06840369	0.60789
OGLE-LMC-DSCT-08548	05 <sup>h</sup> 20 <sup>m</sup> 30 <sup>s</sup> .89	−68°56′09″.4	20.066	20.597	0.07349019	8.6574
OGLE-LMC-DSCT-10144	05 <sup>h</sup> 27 <sup>m</sup> 54 <sup>s</sup> .03	−70°10′55″.0	19.891	20.322	0.05841408	2.34055
OGLE-LMC-DSCT-12588	05 <sup>h</sup> 40 <sup>m</sup> 47 <sup>s</sup> .14	−68°15′25″.0	19.860	20.324	0.07365487	5.0079
OGLE-LMC-DSCT-13577	05 <sup>h</sup> 49 <sup>m</sup> 02 <sup>s</sup> .91	−67°37′37″.3	18.935	19.616	0.09116738	44.202
OGLE-LMC-DSCT-14681	06 <sup>h</sup> 01 <sup>m</sup> 37 <sup>s</sup> .06	−70°37′30″.6	19.219	19.962	0.06718554	19.244
OGLE-LMC-DSCT-15715	06 <sup>h</sup> 50 <sup>m</sup> 22 <sup>s</sup> .94	−79°20′23″.8	14.803	15.674	0.07711367	4.9700

## 11. Summary

We presented the OGLE collection of about 15 000  $\delta$  Sct variables in the LMC. Approximately, two-thirds of these stars represent new discoveries. This compilation constitutes the most extensive sample of extragalactic  $\delta$  Sct stars published to date. Our catalog is a part of the OCVS, which presently comprises around 1.1 mil-

<sup>§</sup><https://alexiosliakos.weebly.com/catalogue.html>

lion manually selected and classified variable stars in the Milky Way and the Magellanic Clouds. The OCVS facilitates comparative research on pulsating stars in different stellar environments. The extensive and well-sampled OGLE light curves in the standard photometric system offer opportunities to investigate exotic modes in pulsating stars, assess the stability of periods, and detect pulsating stars in binary systems.

This paper provides just a glimpse of the potential research that can be carried out on the variables within our collection. We presented the on-sky distribution of  $\delta$  Sct stars in the Magellanic System, derived empirical PL relations for fundamental-mode and first-overtone pulsators and compared them to the PL relations for classical Cepheids. Additionally, we conducted a comparison of period ratios in multimode  $\delta$  Sct variables originated from the Milky Way and the Magellanic Clouds. Finally, we reported the discovery of the first-known candidates for extragalactic eclipsing binaries containing a  $\delta$  Sct component.

**Acknowledgements.** This work has been funded by the National Science Centre, Poland, grant no. 2022/45/B/ST9/00243. For the purpose of Open Access, the author has applied a CC-BY public copyright license to any Author Accepted Manuscript (AAM) version arising from this submission.

## REFERENCES

- Barac, N., Bedding, T.R., Murphy, S.J., and Hey, D.R. 2022, *MNRAS*, **516**, 2080.
- Breger M. 2000, *ASP Conf. Ser.*, **210**, 3.
- Christy, C.T., Jayasinghe, T., Stanek, K.Z., *et al.* 2023, *MNRAS*, **519**, 5271.
- Clementini, G., Ripepi, V., Garofalo, A., *et al.* 2023, *A&A*, **674**, A18.
- Cohen, R.E., and Sarajedini, A. 2012, *MNRAS*, **419**, 342.
- Gaia Collaboration, De Ridder, J., Ripepi, V., *et al.* 2023, *A&A*, **674**, A36.
- Garg, A., Cook, K.H., Nikolaev, S., *et al.* 2010, *AJ*, **140**, 328.
- Jacyszyn-Dobrzaniecka, A.M., Skowron, D.M., Mróz, P., *et al.* 2016, *Acta Astron.*, **66**, 149.
- Jacyszyn-Dobrzaniecka, A.M., Skowron, D.M., Mróz, P., *et al.* 2017, *Acta Astron.*, **67**, 1.
- Jayasinghe, T., Stanek, K. Z., Kochanek, C. S., *et al.* 2019, *MNRAS*, **485**, 961.
- Jayasinghe, T., Stanek, K.Z., Kochanek, C.S., *et al.* 2020, *MNRAS*, **493**, 4186.
- Kaluzny, J., and Rucinski, S.M. 2003, *AJ*, **126**, 237.
- Kim, D.-W., Protopoulos, P., Bailer-Jones, C.A.L., *et al.* 2014, *A&A*, **566**, A43.
- Liakos, A., and Niarchos, P. 2017, *MNRAS*, **465**, 1181.
- Martínez-Vázquez, C.E., Salinas, R., Vivas, A.K., and Catelan, M. 2022, *ApJ*, **940**, L25.
- McNamara, D.H., Clementini, G., and Marconi, M. 2007, *AJ*, **133**, 2752.
- McNamara, D.H. 2011, *AJ*, **142**, 110.
- Nemec, J.M., Linnell Nemec, A.F., and Lutz, T.E. 1994, *AJ*, **108**, 222.
- Netzel, H., Pietrukowicz, P., Soszyński, I., and Wrona, M. 2022, *MNRAS*, **510**, 1748.
- Ngeow, C.-C., Bhardwaj, A., Graham, M. J., *et al.* 2023, *AJ*, **165**, 190.
- Petersen, J. O., and Christensen-Dalsgaard, J. 1996, *A&A*, **312**, 463.
- Pietrukowicz, P., Soszyński, I., Netzel, H., *et al.* 2020, *Acta Astron.*, **70**, 241.
- Pietrzyński, G., Graczyk, D., Gallenne, A., *et al.* 2019, *Nature*, **567**, 200.
- Poleski, R., Soszyński, I., Udalski, A., *et al.* 2010, *Acta Astron.*, **60**, 1.
- Poretti, E., Suárez, J.C., Niarchos, P.G., *et al.* 2005, *A&A*, **440**, 1097.

- Rest, A., Stubbs, C., Becker, A.C., *et al.* 2005, *ApJ*, **634**, 1103.
- Ripepi, V., Chemin, L., Molinaro, R., *et al.* 2022, *MNRAS*, **512**, 563.
- Ripepi, V., Clementini, G., Molinaro, R., *et al.* 2023, *A&A*, **674**, A17.
- Salinas, R., Pajkos, M.A., Vivas, A.K., Strader, J., and Contreras Ramos, R. 2018, *AJ*, **155**, 183.
- Schwarzenberg-Czerny, A. 1996, *ApJ*, **460**, L107.
- Skowron, D.M., Skowron, J., Udalski, A., *et al.* 2021, *ApJS*, **252**, 23.
- Soszyński, I., Udalski, A., Szymański, M., *et al.* 2003, *Acta Astron.*, **53**, 93.
- Soszyński, I., Poleski, R., Udalski, A., *et al.* 2008, *Acta Astron.*, **58**, 163.
- Soszyński, I., Udalski, A., Szymański, M.K., *et al.* 2015a, *Acta Astron.*, **65**, 297.
- Soszyński, I., Udalski, A., Szymański, M.K., *et al.* 2015b, *Acta Astron.*, **65**, 329.
- Soszyński, I., Udalski, A., Szymański, M.K., *et al.* 2016, *Acta Astron.*, **66**, 131.
- Soszyński, I., Udalski, A., Szymański, M.K., *et al.* 2017, *Acta Astron.*, **67**, 103.
- Soszyński, I., Udalski, A., Szymański, M.K., *et al.* 2019, *Acta Astron.*, **69**, 87.
- Soszyński, I., Udalski, A., Szymański, M.K., *et al.* 2020, *Acta Astron.*, **70**, 101.
- Soszyński, I., Pietrukowicz, P., Skowron, J., *et al.* 2021, *Acta Astron.*, **71**, 189.
- Soszyński, I., Udalski, A., Skowron, J., *et al.* 2022, *Acta Astron.*, **72**, 245.
- Udalski, A., Szymański, M.K., and Szymański, G. 2015, *Acta Astron.*, **65**, 1.
- Udalski, A., Soszyński, I., Pietrukowicz, P., *et al.* 2018, *Acta Astron.*, **68**, 315.
- Watson, C.L., Henden, A.A., and Price, A. 2006, *Soc. Astron. Sci. Annu. Symp.*, **25**, 47.
- Ziaali, E., Bedding, T.R., Murphy, S.J., Van Reeth, T., and Hey, D.R. 2019, *MNRAS*, **486**, 4348.